arXiv:cond-mat/0501610v2 [cond-mat.soft] 25 Apr 2005

Optical conductivity of wet DNA

A. Hübsch[1], R. G. Endres[2], D. L. Cox[1,3,4], and R. R. P. Singh[1,3]
[1]*Department of Physics, University of California, Davis, CA 95616*
[2]*NEC Laboratories America, Inc., Princeton, NJ 08540*
[3]*Center for Biophotonics Science and Technology, University of California, Davis, CA 95616*
[4]*Center for Theoretical Biological Physics, University of California, San Diego, CA 92119*
(Dated: February 2, 2008)

Motivated by recent experiments we study the optical conductivity of DNA in its natural environment containing water molecules and counter ions. Our density functional theory calculations (using SIESTA) for four base pair B-DNA with order 250 surrounding water molecules suggest a thermally activated doping of the DNA by water states which generically leads to an electronic contribution to low-frequency absorption. The main contributions to the doping result from water near DNA ends, breaks, or nicks and are thus potentially associated with temporal or structural defects in the DNA.

PACS numbers: 87.14.Gg, 87.15.Aa, 87.15.Mi

The electronic properties of DNA have received considerable scientific attention in the last few years, motivated both by possible use in molecular electronics [1] and by speculation that electronic processes can speed up the location (and possibly repair) of damage sites in living cells [2]. A number of experiments have studied conductance of DNA in different contexts (for a recent review see Ref. 3). Of particular note have been observations of activated behavior with small gaps, of order 0.1-0.3 eV [4, 5], which stand in contrast to the peak optical absorption of DNA in the ultraviolet at 3.5-4 eV. Evidently, such small activation energies, if not extrinsically induced, require an intrinsic doping mechanism.

To address this issue, we study several DNA tetramers surrounded by waters and counterions using a combination of classical molecular dynamics (MD) with density functional theory (DFT) employing the local basis set SIESTA code [6]. To our knowledge, this is the first time that the electronic conductivity of DNA has been computed with a full quantum mechanical treatment of water and counterions in a dynamically fluctuating environment, although similar methods have been used before to study charge migration in DNA [7, 8] *without* explicit quantum treatment of the environment. Our tetramers are in the fully hydrated biological form (B-DNA), with order 250 water molecules. We find evidence that waters in contact with DNA bases can dope the DNA with excitation gaps as small as 0.1-0.3 eV. We find absorption at low frequencies in agreement with optical experiments [5] if we increase the number of bases exposed to water. In a cellular environment, these will be associated with temporal or structural defects, but in many solid-state experiments can also arise from the flattening and unwinding of the DNA helix.

We also study the peak absorption in DNA in the ultraviolet at 3.5-4 eV. The calculated frequency dependent conductivity agrees well with the measured peak absorption for λ-phage DNA[5]. While the peak location is found to be stable, there are distinct features near the peak, which vary with DNA sequence and different environmental configurations accessed during a typical MD run. Within the time scales of the MD (out to 1 ns), our calculations are unable to uniquely determine sequence specificity, but some specificity/fingerprinting may be possible with signal averaging.

These results confirm that while the DNA is a large-gap material, environmental conditions can induce states in the gap, which can in turn lead to a small but non-zero sub-gap absorption. Such states are also crucial for understanding room temperature thermally activated electron dynamics in the DNA, a mechanism that has gained wide acceptance for observed long-range electron transfer in DNA[1].

Electronic structure calculations have previously been performed for dry A-DNA [9] and for crystallized Z-DNA [10] where the effects of solvent and counterions were also addressed. Here, we extend our recent work [11] by considering dynamical fluctuations of the environment. Other efforts have been made to study electronic spectra of DNA in fluctuating environments both without [12] and with [7, 8] counterions and water. Our work differs from these latter efforts by the explicit quantum mechanical treatment of water and counterion states.

To calculate the electronic spectra and optical conductivity we have used the fully ab initio DFT code SIESTA [6]. It uses Troullier-Martins norm-conserving pseudo potentials [13] in the Kleinman-Bylander form [14]. We have used the generalized gradient approximation (GGA) for the exchange-correlation energy functional in the version of Perdew, Burke, and Ernzerhof [15]. SIESTA uses a basis set of numerical atomic orbitals where the method by Sankey and Niklewski [16] is employed. For the DNA we have used a double-ζ basis set except for phosphorus and the counterions for which the polarization orbitals are also included. For the surrounding water molecules (about 250) we have only used the minimal, single-ζ basis set.

The optical conductivity is given by the Kubo formula

$$\sigma_{1,\mu}(\omega) = \pi \frac{e^2}{V} \frac{1-e^{-\beta\hbar\omega}}{\omega} \times \sum_{n,m} \frac{e^{-\beta\varepsilon_n}}{Z} \delta\left(\varepsilon_n - \varepsilon_m - \hbar\omega\right) \left|\langle n| j_\mu |m\rangle\right|^2$$

and depends on the frequency ω. Here, ε_n, ε_m and $|n\rangle$, $|m\rangle$ are the energies and wave functions of the DFT Hamiltonian, respectively. V denotes the unit cell volume, and j_μ with $\mu = \perp, \parallel$ is the component of the current operator perpendicular or parallel to the DNA strand direction. The conductivity computed here does not include time dependent DFT or scissors corrections.

The solvated DNA structures were obtained from classical MD simulations with the AMBER7 package [17] (parm98 force field). The four base-pair long DNA structures (B-DNA 5'-GAAT-3', 5'-GGGG-3', 5'-AAAA-3', and TT-dimer) were initially charge-neutralized with counterions (either by 6 Na^+ or 3 Mg^{2+}) and solvated with about 600 TIP3P water molecules. A simulation box of dimensions $38\times35.4\times25\mathring{A}^3$ (z-axis parallel to DNA axis) with periodic boundary conditions was applied. After equilibration at room temperature for 1 ns, the trajectory was recorded every 10 ps over a simulation time of 1 ns. The resulting 100 snapshots were used for subsequent analysis. All simulations employed the SHAKE method to fix hydrogen-heavy atom distances allowing a 2 fs integration time step. The cut-off for long-range interactions was set to 10 $\mathring{A}$. TT-dimer (segment 5'-ATTA-3' from PDB code 1SM5) was further constrained using the BELLY option to preserve the distorted DNA structure.

To use the structures from MD simulations in DFT calculations we had to reduce the number of atoms. We only kept the first and second solvation shell (approximately 30 water molecules per nucleotide) so that all water molecules within a 4.7 Å radius were included. We incorporated about 1000 atoms in our DFT calculation so that the computations were quite time consuming. In particular, the evaluation of the optical conductivity was very expensive. To speed up the computations we restricted the number of included unoccupied states which only affect the high-energy spectra above 5 eV. The calculation of optical conductivity for a given structure snapshot took about 5 days on AMD's Opteron CPU where approximately 2 GB RAM was needed. All calculations were done at room temperature.

In order to identify the energetically important states near the Fermi energy, we projected the density of states (DOS) on the atomic p_z orbitals of the base pairs and on the water molecules. We also calculated the projected DOS of the counterions, phosphates, and the sugars. However, we only found contributions of the p_z orbitals and the water molecules near the Fermi level. A typical projected DOS of structure snapshot of a 5'-GAAT-3' sequence with Mg counterions is shown in Fig. 1. As seen in panel (a), there is a rather large π-π^* gap of about 2.7 eV. However, if we project the DOS on a single base

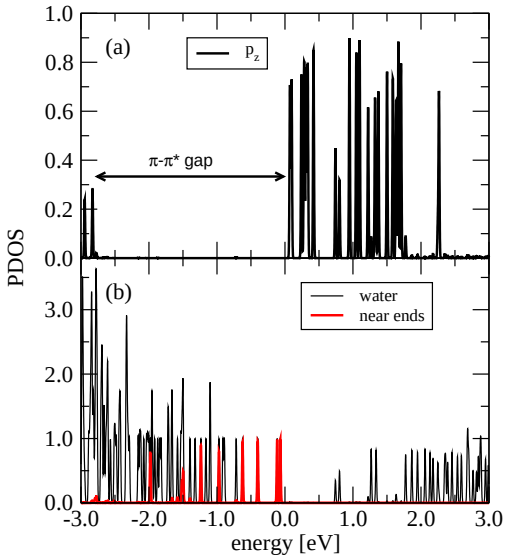

FIG. 1: Typical PDOS of a structure snapshot of a 5'-GAAT-3' sequence with Mg counterions. Panel (a) shows the p_z orbitals of atoms in base pairs. Panel (b) contains the PDOS of all water molecules (thin black line) where the contributions of water molecules near the sequence ends are plotted by a thick red line. The Fermi energy is set to 0.0 eV.

we would find an intrabase π-π^* gap of about 3.7 eV. It turns out that only such intrabase transitions have large dipole matrix elements. Therefore, we observe optical gaps of the same size (compare Figs. 2 and 3).

Although a rather big π-π^* gap is observed the actual gap between the highest occupied molecular orbital (HOMO) and the lowest unoccupied molecular orbital (LUMO) of about 150 meV is very small [combine panels (a) and (b) of Fig. 2]. Thus, electrons could be excited from water states below the Fermi energy into unoccupied p_z orbitals due to thermal fluctuations. Notice that the water states just below the Fermi energy belong to water molecules near the ends of the sequence [see panel (b) of Fig. 1]. Therefore, a small gap between HOMO and LUMO only appears if water molecules could enter the DNA structure on damage sites like ends, breaks, or nicks to contact the DNA bases.

The results of the projected DOS suggest the possibility of a thermally activated doping of the DNA by water states which should also lead to an electronic contribution to the low-frequency absorption. We indeed observe low-energy features in the optical conductivity [panel (a) Fig. 2]. By studying the (fictitious) temperature dependence of these features within SIESTA, we confirm that they are due to transitions between thermally occupied π^* states of the DNA bases. Furthermore, as shown in panel (b), we also observe the pronounced π-π^* transition at 3.8 eV. Whereas the polarization dependence of the low-energy absorption is rather small [see panel (a)] the in-plane π-π^* transition is much more visible if the elec-

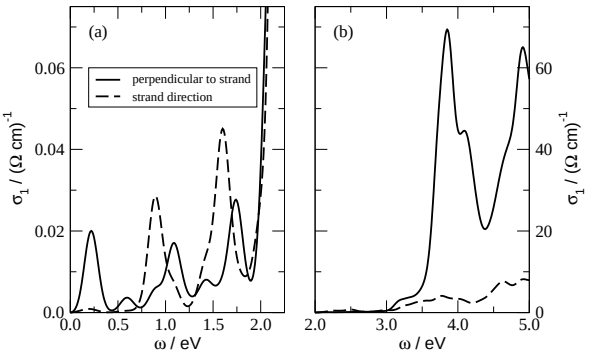

FIG. 2: Polarization dependence of the optical conductivity for a structure snapshot of a 5'-GAAT-3' sequence with Na counterions where $\sigma_{1,\perp}(\omega)$ $[\sigma_{1,\parallel}(\omega)]$ is plotted with solid [dashed] lines. Panel (a) shows the low-energy features whereas panel (b) presents the range of the π-π^* transition. The theoretical line spectra are broadened with Gaussian functions of width 0.1 eV.

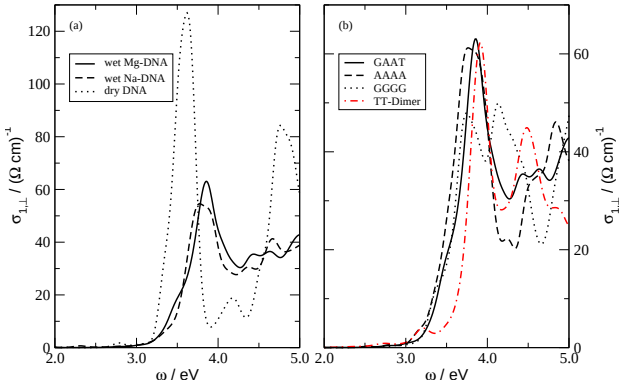

FIG. 3: Robustness of the π-π^* transition regarding environment and DNA sequence. Panel (a) shows the effects of the surrounding water molecules and counterions on the optical conductivity of a 5'-GAAT-3' sequence. The results for different B-DNA sequences in a wet environment containing Mg counterions are compared in panel (b). The spectra for the wet 5'-GAAT-3' (5'-AAAA-3', 5'-GGGG-3', and TT-dimer) sequences have been averaged over the results of 9 (5) structure snap shots. The theoretical line spectra are broadened with Gaussian functions of width 0.1 eV.

tric field is perpendicular to the DNA strand direction. A less pronounced anisotropy of the optical conductivity has also been found in Ref. 10.

To take into account the dynamical character of the environment we average the results for the optical conductivity over up to 9 structure snapshots from the MD simulations. As discussed above, the low-energy features of the optical conductivity result from a doping of the DNA by water states. Therefore, they are strongly affected by environment fluctuations and we only obtain some smeared intensity in the low-energy range of the averaged conductivity. In contrast, the intrinsic π-π^* gap is much less affected by dynamical fluctuations leading to well defined structures in that range.

Due to the intrinsic character of the π-π^* transition the averaged optical conductivity in the range $2-5$ eV is barely affected by different counterions [see panel (a) of Fig. 3]. To show that the main structure in the spectra around 3.7 eV really has to be interpreted as the intrabase π-π^* transition we also plot the optical conductivity of dry protonated B-DNA in panel (a) of Fig. 3. Although the spectra of wet and dry B-DNA considerably differ in the intensities, the peak positions agree quite well. Furthermore, as seen from panel (b) of Fig. 3, peak position and shape of the π-π^* transition depend only weakly on sequence whereas remarkable differences are observed in the range $4-5$ eV.

In Fig. 4 we compare our results with recent optical experiments [5] and find a nice agreement for the range of the π-π^* transition above $10000\,cm^{-1}$. However, we find pronounced polarization dependence of the conductivity (see Fig. 2) whereas the experimental spectra are almost isotropic. The latter can be explained by substantial variations in the axis of the macroscopically orientated DNA duplex [5].

The spectra below $500\,cm^{-1}$ are also affected by vibrational modes of the double helix structure and the surrounding water molecules, which are not included in our DFT calculations. In particular, the optical conductivity below $100\,cm^{-1}$ has been interpreted in Ref. 18 as a pure water dipole relaxation. However, our DFT calculations clearly show an electronic conductivity even at very low frequencies (see Fig. 4). As already discussed above, the low-frequency conductivity results from a doping of the DNA by water molecules near the bases. Therefore, the theoretically observed conductivity at low frequencies, which is approximately an order of magnitude smaller than the experimental values, would be further increased if more waters could enter the DNA structure on additional damage sites like ends, breaks, or nicks.

A striking aspect of the work of Briman *et al.* is the near identity of the microwave conductivity for single stranded and double stranded DNA [18]. This, as well as the order of magnitude discrepancy between our low frequency calculations and their data can possibly be resolved as follows: (i) We have order one water per tetramer associated with end bases; if this is upped to one level per base we gain a factor of eight in absorption intensity, close to that needed to resolve the discrepancy with the Briman *et al.* data. This is plausible for single stranded DNA adsorbed to the sapphire substrate of Ref. 18. (ii) To get the same low frequency conductivity contribution for double stranded DNA requires that the DNA flatten and unwind (the helix) as has been observed elsewhere for DNA on surfaces [19]. In the unwound configuration the extra space between bases allows for entry by water molecules. Obviously some of the microwave absorption will be caused by water motion alone as suggested by Ref. 18; our purpose here is to note that electronic absorption affiliated with defect states can be

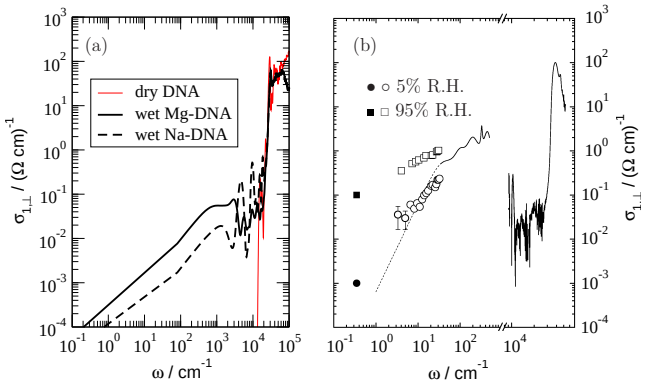

FIG. 4: Panel (a) is a log-log plot of the optical conductivity from Fig. 3, panel (a). Panel (b) shows experimental data for DNA in a 5% and 95% relative humidity environment taken from Ref. 5.

comparable.

A grand technological challenge of our times is to develop a rapid scheme for sequence differentiation in DNA, for example to be able to differentiate between alleles of a given gene. Current technologies, such as those of real-time or quantitative PCR, rely on fluorescent dyes and the FRET (Fluorescent Resonance Energy Transfer) method. This requires developing gene specific labeling dyes, or donors and acceptors, which will lead to fluorescent signals reflecting the amount of a given double-stranded DNA sequence in the system. However, the intrinsic electronic [21] and optical properties of DNA also vary with sequence. So, a natural question is: would it be possible to develop label-free optical fingerprinting of DNA that would allow one to infer different alleles directly from optical experiments without the use of dyes?

Optical fingerprinting would require two things to happen. First, one would need optical signatures predominantly from a given gene and one would need signals from different alleles to be sufficiently different. The former may be achieved by gene-chip and by surface enhancement techniques. We can address here the latter question, how different are the spectra from different sequences and consequently how easy would it be to establish such a difference experimentally. Clearly the spectra from different sequences strongly overlap and this makes it harder to distinguish them. Having large copies of the gene generated through polymerase chain reaction will lead to signal averaging and the time averaged signal can be distinguished if there is sufficient accuracy. For example, we have about 30% statistical variance for five configurations used in averaged conductivity calculations of tetramers while the means diverge at the $\approx 5\%$ level. Hence, we could expect single point frequency sampling to discern the sequences here with a configuration increase to 180. This number could likely be reduced with judicious use of multipoint frequency sampling. If a simple definitive fingerprint is required without full sequence information, as might be appropriate in applications in forensics or pathogen detection, numbers in the ballpark of 100-1000 clones of a given sequence could be sufficient. This compares with the $10^5 - 10^6$ levels of clones necessary for current state of the art DNA sequencing technology[20]. Quantitative theoretical studies will be an important aid in developing such technologies.

We thank G. Grüner for the permission to use the plot of the experimental data from Ref. 5. This work was supported by NSF grant PHY 0120999 (the Center for Biophotonics Science and Technology) and DMR-0240918, by the US Department of Energy, Division of Materials Research, Office of Basic Energy Science, and by DFG grant HU 993/1-1. DLC is grateful for the support of the Center for Theoretical Biological Physics through NSF grants PHY0216576 and PHY0225630, and the J.S. Guggenheim Memorial Foundation.

[1] C. Dekker and M.A. Ratner, Phys. World **14**, 29 (2001), M. Di Ventra and M. Zwolak, in *Encyclopedia of Nanoscience and Nanotechnology*, edited by H. Singh-Nalwa (American Scientific Publishers, 2004).
[2] E.M. Boon *et al.*, Proc. Nat. Acad. Sci. (USA) **100**, 12543 (2003).
[3] R. G. Endres *et al.* Rev. Mod. Phys. **76**, 195 (2004).
[4] K.-H. Yoo *et al.*, Phys. Rev. Lett. **87**, 198102 (2001).
[5] E. Helgren *et al.*, cond-mat/0111299.
[6] D. Sánchez-Portal *et al.*, Int. J. Quantum Chem. **65**, 453 (1997); E. Artacho *et al.*, Phys. Status Solidi (b) **215**, 809 (1999); P. Ordejón *et al.* Phys. Rev. B **53**, R10441 (1996).
[7] R.N. Barnett *et al.*, Science **294**, 567 (2001).
[8] A. Troisi and G. Orlandi, J. Phys. Chem. B**106**, 2093 (2002).
[9] P. J. de Pablo *et al.*, Phys. Rev. Lett. **85**, 4992 (2000).
[10] F. L. Gervasio, *et al.* Phys. Rev. Lett. **89**, 108102 (2002).
[11] R. G. Endres *et al.* cond-mat/0201404.
[12] J.P. Lewis *et al.*, Phys. Stat. Sol. B**233**, 90 (2002).
[13] N. Troullier and J. L. Martins, Phys. Rev. B **43**, 1993 (1991).
[14] L. Kleinman and D.M. Bylander, Phys. Rev. Lett. **48**, 1425 (1982).
[15] J. P. Perdew *et al.* Phys. Rev. Lett. **77**, 3865 (1996).
[16] O. F. Sankey and D. J. Niklewski, Phys. Rev. B **40**, 3979 (1989).
[17] D. A. Case *et al.*, AMBER 7, University of California, San Francisco (2002).
[18] M. Briman *et al.*, Nano Lett. **4**, 733 (2004).
[19] T. Kanno *et al.* Appl. Phys. Lett. **77**, 3848 (2000); L. Cai *et al.* Nanotechnology **12**, 211 (2001).
[20] J.C. Venter *et al.*, Science **280**, 1540 (1998).
[21] M. Zwolak and M. Di Ventra, Nano Lett. **5**, 421 (2005).